

# Investigations on the Behaviour of Transverse Steel Reinforcement with Low Dosage Nano-Silica

<sup>1</sup>P. Rahamatulla, <sup>2</sup>G. S. Harish Kumar

<sup>1,2</sup> Assistant Professor, Department of Civil Engineering, Ashoka Women's Engineering College,  
Kurnool, Andhra Pradesh, India

## Article Info

Page Number: 420 - 425

Publication Issue:

Vol 69 No. 1 (2020)

## Abstract

This study investigates the behavior of lightweight aggregate concrete columns using transverse steel reinforcement. Twelve reinforced specimens were subjected to tests with an axial compressive load that gradually and monotonically increased over time. The research looked into two things: tie configurations and transverse steel. The fracture patterns of constrained lightweight aggregate concrete columns were significantly different from those of normal weight concrete specimens. Some researchers have suggested that the contact between coarse aggregate and cement paste is where failure planes may have traveled or evolved. By carefully selecting the tie pattern and providing appropriate steel reinforcement, lightweight aggregate concrete can be made to be extremely flexible and durable. Throughout the test, it is discovered that specimens housed in rectangular hoops with cross ties have adequate axial load-carrying capacity and ductility. An analytical model has been proposed that incorporates both the confinement efficiency factor ( $I_t$ ) and a coefficient ( $k$ ) in order to accurately estimate peak stress and strain. The model is very accurate at predicting the future when compared to other models

Article Received: 12 September 2020

Revised: 16 October 2020

Accepted: 20 November 2020

Publication: 25 December 2020

## 1. INTRODUCTION

Increased seismic resistance capacity of building structures, as well as a decrease in dead weight and component dimensions, are among the many well-known advantages of LWAC. Other benefits include increased fire resistance and reduced permeability. <sup>1,2</sup> As a result, it is used extensively in bridges and high-rise structures, and its potential applications appear promising. Although LWAC's lower elastic modulus and high shear brittleness prevent it from being utilized in significant vertical bearing components like columns, it is still widely used in other applications. Consequently, the vertical bearing components play a crucial role in preventing building structures from ever collapsing. A reasonable lateral confinement is generally recommended in order to successfully increase column toughness.

Over the course of the past four decades, a number of studies have been conducted on the behavior of NWC columns that are subjected to concentric loads. Numerous parameters were examined in depth, including the concrete compressive strength ( $f_{c0}$ ), tie yield strength ( $f_{yt}$ ), type of tie used ( $s$ ), length of tie used ( $rg$ ), and amount of concrete used ( $cov$ ), for example. <sup>6</sup> Park et al.<sup>7</sup>, Valens et al.<sup>8</sup>, and Fajitas and Shah have also proposed stress-strain models for lateral-constrained NWC specimens. <sup>9</sup> These models may not accurately represent LWAC columns with transverse steel reinforcing beams based on genuine NWC data. The stress-strain behavior of passive or active

restricted concrete columns has been the subject of numerous recent studies. It is necessary to investigate the entire stress–strain curve of the confined material in order to evaluate the structural components made of reinforced concrete's deformability, ductility, and strength. The axial compressive behavior of LWAC columns under confinement has only been the subject of a limited number of experiments. Limited LWAC's behavior under stress and strain has not yet been thoroughly studied. Martinez et al. found correlations between the maximum stress, maximum strain, and ductility ratio. under concentric loading, studied 27 LWAC columns enclosed in circular spirals. Basset and Suzumori examined restricted high-strength LWAC in full-size columns with various parameters. When subjected to long-term loading, Berkley and colleagues' research revealed that confined LWAC columns had significantly different properties than unconfined specimens. Using an experiment utilizing eight high-strength LWAC columns encased in composite elliptical spirals, Kahlo and Bozorgzadeh<sup>15</sup> developed a stress–strain model based on peak stress and peak strain calculation formulas. Haling et al. discovered wider stirrups and smaller tie spacing. to significantly improve specimens' capacity for deformation in confined conditions. The problem of calculating the elastic modulus of LWAC has finally been solved. The axial compression of constrained LWAC columns has received less research attention, according to a comprehensive review of the existing literature. It is generally agreed that previous studies have relied on the NWC specimens for their theoretical analysis, but that these studies have not provided sufficient experimental support or a clear theoretical foundation.

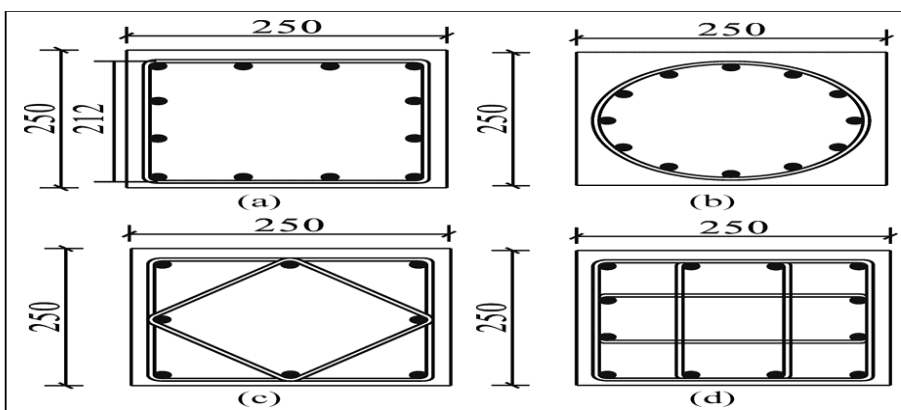


**Figure 1. Cross-sectional dimensions for specimens: series A, (b) series B, (c) series C; (d) series D.”**

## 2. LITERATURE REVIEW

The test setup is shown in Figure 2. All specimens were loaded at a loading rate of 0.01 millimeters per second (0.012 inches per second) on a universal testing machine in displacement-controlled mode. A coating of fine sand three millimeters thick was applied to the column's ends on both ends as a cap to ensure a consistent weight distribution throughout the column's cross section. This week, an upper column capping device with a 20-mm steel plate thickness and a 150-mm steel plate height was installed to improve local confinement and prevent early concrete crushing (see Figure 4). A spherical hinge at the lower end of the column was another safety measure used to maintain uniform compression pressure. The test was declared terminated and the results were recorded when the specimen's axial load-carrying capacity dropped below 60% of the maximum load. Each specimen displayed a consistent behavior pattern during the first loading stage. Since the axial

compressive load was primarily supported by the concrete and longitudinal bars at the time, lateral confinement had little effect on it. The concrete cover did not appear to have any cracks. During the linear elastic phase of the LWAC specimens' deformations, lateral reinforcement stresses and Poisson ratio values were relatively low. The concrete coating began to peel away from the foundation as the load increased, creating vertical fissures along the corner longitudinal bars. The specimens then reached their ultimate state. The failure appearance and fracture patterns of two typical specimens, the CH-1.97-55 and the BS-1.97-50, were examined using three distinct loading stages (see Fig. 6) shown.

On the specimen CH-1.97-55, an intriguing phenomenon did not emerge until a load of 1300 kN (or roughly 58% of the peak load,  $P_{test}$ ) was applied. The sound of concrete cracking shortly thereafter indicated that internal fractures were beginning to form. At 1600 kN, the top ends of specimen surfaces B and C fractured at 0.2 mm width and 1 cm length (approximately 72%  $P_{test}$ ). When the load was increased to 1850 kN and 2100 kN, respectively (corresponding to 83 and 95 percent  $P_{test}$ ), there were vertical fractures that were 5 cm long on both surfaces A and B of the specimen. As can be seen in the figure, while surface B's horizontal and vertical cracks continued to diminish, surface A's vertical and diagonal cracks continued to grow. Figure 2 shows the lateral reinforcing strain distribution along the column height after the specimens had reached their maximum stresses and the peak stress had been reduced by 15%. This was followed by a loud cracking sound. The decreased expansion of the core concrete during the initial loading stage was cited as the reason for the lower lateral steel strains. Concrete cracking reveals the structure of the column's ties more clearly. In this investigation, crack occurrence and development were significantly different between NWC and LWAC specimens. Two of the main reasons for this are the higher interfacial strength of LWAC and steel reinforcement. Consequently, with the exception of BS-2.80-35, the ties did not reach their yield point at full load in any of the examples. As a result of the concrete cover spalling over a large area and the formation of failure planes, stresses on the numerous steels in the failure zone quickly increased. The stirrups in the failure planes gave way, indicating that the axial force should be reduced to 85% of its maximum value at this point. Due to inadequate confinement provided by the lateral reinforcements, specimens with lower ratios of lateral reinforcements to core concrete experienced crush damage earlier

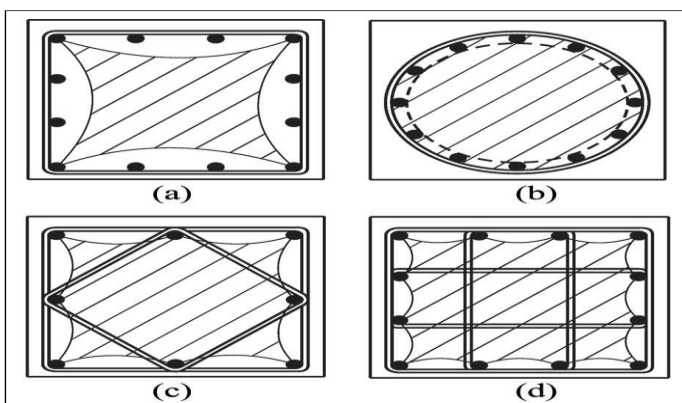


**Fig 2: Effectively confined area of core concrete:(a)seriesA,(b)seriesB,(c)seriesC,and(d)seriesD.**

### 3. PROPOSED SYSTEM

Figure 2 depicts the compression and flexibility of non-prewetting LWAC samples when there were no significant differences in compression strength between samples containing nano-SiO<sub>2</sub> and those omitting it (25.2 MPa). At 3.5 MPa, the flexural strength is comparable to that of the control sample (3.3 MPa). The compressive and flexural strengths reached their maximums when 0.1 percent nano-SiO<sub>2</sub> was added. When compared to the control sample, we found that the 7-day compressive and flexural strengths increased by 40% and 18%, respectively.

When the dose was increased, nano-SiO<sub>2</sub> increased compressive and flexural strength by 0.2-0.5%; When nano-SiO<sub>2</sub> was added, the correlation was found to decrease by 1%. [ weight percent] When the dose was just 0.2%, the 7-day compression and flexural strengths showed an increase of 24% and 6% over the control samples, respectively. However, when the dose was 0.1 wt percent, they both decreased in effectiveness by approximately 11%. A weight-percentage dose increase of 0.5 was used to achieve 7-day compressive and flexural strengths of 32.4 and 3.6 MPa. When the dosage reached 1%, both compressive and flexural strength decreased significantly. Similar to those of the control samples, these outcomes were nearly identical..

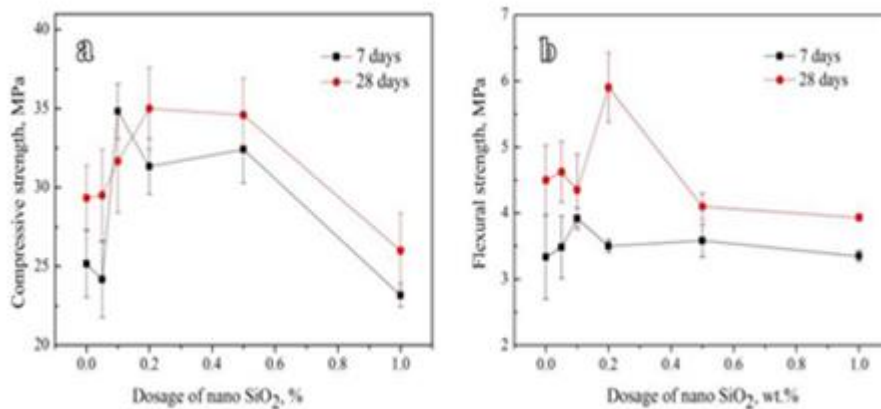


**Figure 3. “Properties of non-prewetting lightweight concrete (7 and 28 days) as a function of nano-SiO<sub>2</sub> dose (a) compression strength and (b) flexural strength.” SiO<sub>2</sub>:**

When the dose was increased to 0.05 weight percent, compression and flexural strength were 30 and 4.5 MPa, respectively. At a dose of 0.2 percent, the highest compression and flexibility strengths of 35 and 5.9 MPa could be achieved. When the dosage was increased from 0.5 to 1%, the 28-day specimens' compressive and flexural strengths were significantly reduced.

Figure 3 depicts the compressive and flexural strengths of prewetting LWAC samples seven and 28 days after curing. Increases in nano-SiO<sub>2</sub> dosage did not result in a linear increase in compressive or flexural strength, as shown in this figure. A similar trend can be observed in the compressive and flexural strengths of samples that have not been pre-soaked in water. The compressive strength of the nano-SiO<sub>2</sub> sample after seven days was the same as that of the control sample, 23.1 MPa. It is ideal due to its 2.9 MPa flexural strength of 3.0 MPa. Over the course of seven days, peak compression and flexural strength values of 0.1 weight percent were also observed. After seven days, these specimens had higher compressive and flexural strengths of 40% and 41%, respectively, than the control sample.

When compared to control samples, the compressive and flexural strengths do not significantly differ after seven days at nano-SiO<sub>2</sub> presetting concentrations of 0.2 percent and 0.5 percent weight

percent, respectively. This area experienced a lot of movement, but it eventually settled at 1%. When compared to the controls, the seven-day compressive and flexural strengths at a dosage of Pressure increased by 24%, but when the dose was decreased by 1%, they decreased by 14%. Two instances. With a dose increase of 0.5 weight percent from the initial dosage level, additional increases of 31.4 percent and 3.8 percent in the 7-day cumulative and flexural strengths were observed. When the dosage reached 1%, the samples' compressive and flexural strengths decreased by approximately 2.5 MPa each after seven days, making them comparable to control samples. The prewetted LWAC samples' compressive and flexural strengths at 28 days are shown in Figure 3 as a function of the nano-SiO<sub>2</sub> dosage. As depicted in Figure 3a (a), when the dosage of nano-SiO<sub>2</sub> is increased, the control sample's average compressive strength rises from 26.8MPa to 30.3MPa and 37.3MPa, respectively. In both instances, this increase is less than 1%. After increasing the concentration of nano-SiO<sub>2</sub> from its initial 0.2 percent to 0.5 percent, compressive strength decreased to 34.8 MPa. By increasing the nano-SiO<sub>2</sub> dosage to 1.0 percent, compressive strength was decreased to 31.2 MPa. When the amount of nano-SiO<sub>2</sub> is increased, the flexural strength changes over time. Nano-modified samples needed to be dosed at a rate of 0.5 percent weight percent to achieve flexural strengths of approximately 4.4 and 5.1 MPa at doses of 0.5 percent weight percent and 0.1 percent weight percent, respectively. The control sample's flexural strength was found to be 3.7 MPa. When the nano SiO<sub>2</sub> dose was 1 percent, the flexural strength decreased.

#### 4.CONCLUSION

According to the findings of this study, confined NWC specimens and LWAC columns both fail in the same way before the peak load point. After the peak load point, the concrete covers of LWAC columns were cut off and spalled, reducing their strength. Cracks appeared across aggregates or at the cement paste interface, which is a significant performance difference from NWC specimens. When diagonal penetrating failure lines intersected horizontal axes, we observed 45-degree diagonal penetrating failure lines. Despite their different materials, LWAC and NWC specimens share the same stress–strain curve development law. The knot arrangement may have a significant impact on the ductility and strength of constrained specimens. Even if the core concrete is not adequately contained, it is possible to improve specimen ductility and load-carrying capacity by using rectangular spiral stirrups (section A). If you apply compound-diamond spiral reinforcement to the specimen's lateral side (section C), the load-carrying capacity increases by approximately 60%. Spiral reinforcements in the exterior and internal layers are not working well together. When compared to other specimens, the D-type examples exhibit greater strength and ductility as well as significant confinement of the core concrete

#### REFERENCES

1. Ferrara L, Cortesi L and Ligabue O. Internal curing of con-crete with presaturated LWA: a preliminary investigation.ACISpecialPublication2015;305:12.1–12.12.
2. Bentur A, Igarashi S-I and Kovler K. Prevention of autoge-nous shrinkage in high-strength concrete by internal curingusingwetlightweightaggregates.CemConcrRes2001;31(11):1587–1591.
3. Ferrara L, Caverzan A and Peled A. “Collapsible” light-weight aggregate concrete. Part I: material concept and pre-liminary characterization under static loadings. Mater Struct2016;49(5):1733–1745.

4. Ferrara L, Caverzan A, Nahum L, et al. "Collapsible" light-weight aggregate concrete. Part II: characterization under static and dynamic loadings. *Mater Struct* 2016; 49(5):1747–1760.
5. Uenal O, Uygunoglu T and Yildiz A. Investigation of properties of low-strength lightweight concrete for thermal insulation. *Build Env* 2007; 42(2):584–590.
6. Sayadi AA, Tapia JV, Neitzert TR, et al. Effects of expanded polystyrene (EPS) particles on fire resistance, thermal conductivity and compressive strength of foamed concrete. *Constr Build Mater* 2016; 112:716–724.
7. Senaratne S, Gerace D, Mirza O, et al. The costs and benefits of combining recycled aggregate with steel fibres as a sustainable, structural material. *J Clean Prod* 2016; 112:2318–2327.
8. Suzuki M, Meddah MS and Sato R. Use of porous ceramic waste aggregates for internal curing of high-performance concrete. *Cem Concr Res* 2009; 39(5):373–381.
9. Raithby KD and Lydon FD. Lightweight concrete in highway bridges. *Int J Cem Compos Lightweight Concr* 1981; 3(2):133–146.
10. Nair H, Ozyildirim C and Sprinkel MM. Use of Lightweight Concrete for Reducing Cracks in Bridge Decks. No. FHWA/VTRC16-R14. 2016. Hensher DA. Fiber-reinforced-plastic (FRP) reinforcement for concrete structures: properties and applications. Vol. 11. 42. PA, USA: Elsevier Publishing, 2016.
12. Ranjbar MM and Mousavi SY. Strength and durability assessment of self-compacted lightweight concrete containing expanded polystyrene. *Mater Struct* 2015; 48(4):1001–1011.